Laser and Particle Beams (2007), *25*, 333–337. Printed in the USA.

DOI: 10.1017/S0263034607000146

Nonlocal electron heat flow in high-Z laser-plasmas with radiation transport

M.J. KESKINEN[1] AND A. SCHMITT[2]

[1]Charged Particle Physics Branch, Naval Research Laboratory, Washington, DC
[2]Laser Plasma Branch, Plasma Physics Division, Naval Research Laboratory, Washington, DC

(RECEIVED 4 January 2007; ACCEPTED 26 February 2007)

Abstract

The effects of radiation transport on nonlocal electron heat flow in high Z laser-produced plasmas is studied. Using a Fokker-Planck model for the electron heat flow, which is coupled to a radiation transport model, it is found that radiation transport strongly modifies electron heat transport at the critical surface and in the overdense regions for an aluminum plasma. It is concluded that, without radiation transport effects, the plasma temperature, as computed from Fokker-Planck models, is overestimated in the critical region and underestimated in the overdense region, for high-Z plasmas.

Keywords: Fokker-Planck; High Z; Laser; Radiation; Transport

1. INTRODUCTION

Energy transport in laser-produced plasmas is an important issue in current high energy density plasma research, e.g., inertial confinement fusion (ICF; Sunahara *et al.*, 2003), femtosecond laser interactions with solids (Anwar *et al.*, 2006; Petrov, 2005; Fisher *et al.*, 2005), and laboratory simulations of astrophysical phenomena using lasers. Thermal and superthermal electrons (Sherlock *et al.*, 2006; Nakamura *et al.*, 2006), radiation transport (Xu *et al.*, 2006; Lan *et al.*, 2005), and shocks can all contribute to energy (Khalenkov *et al.*, 2006) and heat transport in laser-produced plasmas. In particular, the physical mechanism for energy transport in high-Z laser plasmas is an important issue since high-Z layers have been proposed to improve implosion symmetry (Obenschain *et al.*, 2002) of ICF targets.

In ICF, laser energy, absorbed in the hot, low density corona, must be effectively conducted toward colder, higher density regions of the target. A large inward heat flux from the critical surface, toward higher density regions, implies that newly heated material at the surface of the cold target will expand outward rapidly leading to large fuel compression. Large compressions can lead to higher fusion gains. Much experimental data have indicated (Yaakobi & Bristow, 1977; Kruer, 1979; McClellan *et al.*, 1980; Malone *et al.*, 1975) that the heat flux is below the flux predicted by classical electron thermal conduction. Strong inhibition of thermal transport below classical thermal conduction seems to exist in both long and short pulse laser deposition and in both high and low Z targets. In addition, the measured heat transport seems to be reduced, both inward toward higher density regions and laterally toward the exterior.

Several models have been advanced to explain the reduced heat flux in ICF experiments, e.g., ion acoustic turbulence (Bickerton, 1973; Manheimer, 1977; Gray & Kilkenny, 1980), direct current magnetic field effects (Straus *et al.*, 1984), and kinetic theory in steep temperature gradients (Bell *et al.*, 1981; Matte & Virmont, 1982; Luciani *et al.*, 1983; Albritton, 1983; Matte *et al.*, 1984; Bell, 1985; Albritton *et al.*, 1986; Epperlein *et al.*, 1988; Rickard *et al.*, 1989; Epperlein & Short, 1991; Epperlein, 1994; Sunahara *et al.*, 2003).

For studies of electron heat flow in steep temperature gradients, Fokker-Planck (FP) models have been used since the collision mean free path can be on the order of the temperature gradient scale length. Previous FP studies have included improved models for collisional effects, as well as inverse bremsstrahlung absorption and ion motion (Luciani *et al.*, 1983; Albritton, 1983; Matte *et al.*, 1984; Bell, 1985; Albritton *et al.*, 1986; Epperlein, 1994; Sunahara *et al.*, 2003). For moderate to high Z plasmas, radiation transport effects need to be included in FP models. For example, emission due to radiative recombination scales as Z^4. However,

Address correspondence and reprint requests to: M. J. Keskinen, Code 6750, Charged Particle Physics Branch, Plasma Physics Division, Naval Research Laboratory, Washington, DC 20375. E-mail: keskinen@ppd.nrl.navy.mil

the inclusion of radiation transport effects on nonlocal FP electron heat flow has not been studied in detail.

The objective of this paper is to study, using an FP approach, nonlocal electron heat flow in laser-produced plasmas including secondary radiation transport effects. It is found that, for aluminum plasmas, radiation transport strongly modifies plasma temperatures in the critical surface, and in the overdense regions due to enhanced radiative heating and cooling. The outline of this paper is as follows. In Section 2, we discuss the basic FP electron heat flow model including secondary radiation transport effects. In Section 3, we present results from the model. Finally, in Section 4, we summarize our results.

2. MODEL

In this section, the FP model used for electron heat transport, including secondary radiation transport effects, is presented.

2.1. Electron heat transport

The FP equation for a fully ionized plasma can be written (Shkarofsky *et al.*, 1966) as follows:

$$\begin{aligned}\frac{\partial f}{\partial t} + \mathbf{v}\cdot\frac{\partial f}{\partial \mathbf{x}} - \frac{e}{m}\left(\mathbf{E} + \frac{1}{c}\mathbf{v}\times\mathbf{B}\right)\cdot\frac{\partial f}{\partial \mathbf{v}} \\ = \zeta\frac{\partial}{\partial \mathbf{v}}\cdot\frac{v^2\mathbf{I} - \mathbf{vv}}{v^3}\cdot\frac{\partial f}{\partial \mathbf{v}} + C_{ee} + S\end{aligned} \quad (1)$$

where f is the electron distribution function, $\mathbf{E}$ and $\mathbf{B}$ are the electric and magnetic fields, $\mathbf{I}$ is the unit tensor, and $\zeta = (2\pi nZe^4/m^2)\ \ln\Lambda$ with n, Z, and $\ln\Lambda$ the density, ion charge state, and Coulomb logarithm, respectively. Here C_{ee} represents electron-electron collisions and S represents all source terms, e.g., laser absorption and radiation transport. For this study, we ignore magnetic field effects and consider a moderate to high Z plasma.

It is assumed that, to lowest order, the electron distribution function f is weakly anisotropic. As a result, we make the standard decomposition (Shkarofsky *et al.*, 1966; Epperlein, 1994) for f:

$$f = \sum_n \mathbf{f}_n\cdot\frac{\mathbf{v}^n}{v^n} \quad (2)$$

For $n = 0, 1, 2$ we have:

$$\frac{\partial f_0}{\partial t} + \frac{v}{3}\frac{\partial}{\partial \mathbf{x}}\cdot\mathbf{f}_1 + \frac{1}{3v^2}\frac{e}{m}\frac{\partial}{\partial v}(v^2\mathbf{E}\cdot\mathbf{f}_1) = C_0 + S_0, \quad (3)$$

$$\begin{aligned}\frac{\partial \mathbf{f}_1}{\partial t} + v\frac{\partial f_0}{\partial \mathbf{x}} + \frac{\mathbf{E}}{m}\frac{\partial f_0}{\partial v} + \frac{2v}{5}\frac{\partial}{\partial \mathbf{x}}\cdot\mathbf{f}_2 + \frac{2e}{5mv^3} \\ \times\frac{\partial}{\partial v}(v^3\mathbf{E}\cdot\mathbf{f}_2) = C_1,\end{aligned} \quad (4)$$

$$\begin{aligned}\frac{\partial \mathbf{f}_2}{\partial t} + v\left(\frac{\partial}{\partial \mathbf{x}}\mathbf{f}_1 - \frac{1}{3}\left(\frac{\partial}{\partial \mathbf{x}}\cdot\mathbf{f}_1\right)\mathbf{I}\right) + \frac{ev}{m}\frac{\partial}{\partial v} \\ \times\left(\frac{\mathbf{E}\mathbf{f}_1}{v} - \frac{1}{3}\frac{\mathbf{E}\cdot\mathbf{f}_1}{v}\mathbf{I}\right) = C_2,\end{aligned} \quad (5)$$

with the e-i and e-e collisional effects given by (Epperlein, 1994; Shkarofsky *et al.*, 1966):

$$C_n = -\frac{n(n+1)}{2}\nu_{ei}f_n + \nu_{ee}v\frac{\partial}{\partial v}\left[f_n I_0^0 + \frac{v}{3}\frac{\partial f_n}{\partial v}(I_2^0 + J_{-1}^0)\right], \quad (6)$$

with

$$I_p^q = \frac{4\pi}{v^p}\int_0^\infty f_q x^{2+p}dx, \quad (7)$$

with

$$J_p^q = \frac{4\pi}{v^p}\int_v^\infty f_q x^{2+p}dx, \quad (8)$$

where $\nu_{ei} = (4\pi\phi ne^4Z^*/m^2v^3)ln\Lambda$, $\nu_{ee} = (4\pi ne^4/m^2v^3)ln\Lambda$, $\phi = (Z^* + 4.2)/(Z^* + 0.24)$, and $Z^* = \langle Z^2\rangle/\langle Z\rangle$. Here, the angle brackets denote an average over all ion species. Using Z^* and ϕ allows the representation of e-i and e-e collisional effects in C_n, n = 1, 2, without using the second term in the definition of C_n in Eq. (6). This is shown to be a good approximation for moderate to high Z plasmas (Bell, 1985). In Eq. (3), $S_0 = S_{IB} + S_{rad}$. Here, S_{IB} represents laser inverse bremstrahllung absorption and S_{rad} describes secondary radiation sources. For S_{IB}, we use the Langdon prescription (Langdon, 1980). For S_{rad}, we take $S_{rad} = (1/n_em_e)(1/4\pi v^4)q_{rad}$ with q_{rad} being the net radiative heating rate.

The current and heat flux are found from Eqs. (3)–(5):

$$\mathbf{J} = -\frac{e}{3}\int v^3\mathbf{f}_1 dv, \quad (9)$$

$$\mathbf{q} = \frac{m}{6}\int v^5\mathbf{f}_1 dv. \quad (10)$$

The electric field $\mathbf{E}$ in Eqs. (3)–(5) is found self-consistently from the zero current condition, i.e., $\mathbf{J} = 0$. Including only Eqs. (3)–(4), taking $f_2 = 0$, using $\mathbf{J} = 0$, and assumimg a Maxwellian for f_0 the standard Spitzer heat flow and thermal conductivity (Spitzer & Harm, 1953) is recovered.

2.2. Radiation transport

The model used to compute q_{rad} and, hence, S_{rad} in Eq. (3) is now presented. In slab geometry, with the laser incident from the z-direction, the fundamental radiative transfer equation can be written (Griem, 1997):

$$\frac{dI_\nu}{dz} = -\kappa_\nu I_\nu + j_\nu, \tag{11}$$

where I_ν is the radiation intensity, κ_ν is the absorption coefficient, and j_ν is the emission rate. In terms of the optical depth τ, where $d\tau = \kappa_\nu dz$, Eq. (11) can be written:

$$\frac{dI_\nu}{d\tau} = S_\nu - I_\nu \tag{12}$$

where $S_\nu = j_\nu/\kappa_\nu$ is the radiation source. Eq. (12) can be solved formally (Griem, 1997):

$$I_\nu(\tau) = I(0)e^{-\tau} + \int_0^\tau S_\nu(\tau')e^{-(\tau-\tau')}d\tau' \tag{13}$$

where I(0) is the intensity at $\tau = 0$.

The net radiative heating rate q_{rad} can be written (More, 1986; Key, 1985; Zel'dovich & Raizer, 1966):

$$q_{rad} = 4\pi\int d\nu\kappa_\nu I_\nu - 4\pi\int d\nu\kappa_\nu S_\nu \tag{14}$$

The first term gives the radiative heating rate and the second term the radiative cooling rate. Depending on the sign of q_{rad}, there will be a net radiative heating ($q_{rad} > 0$) or a net radiative cooling ($q_{rad} < 0$).

To compute q_{rad} in Eq. (14), the spatial and temporal specification of the source S_ν must be specified. The intensity $I_\nu(z)$ can then be found from Eq. (12). Laser heating of the plasma in the vicinity of the critical surface produces radiative emission in both the forward and backward directions. This radiation consists (Duston *et al.*, 1983, 1985) primarily of soft X-ray and XUV photons for aluminum targets. The soft X-rays, with energies above approximately 1.5 keV, are emitted from plasmas with temperatures above about 250 eV, and result from bound-bound transitions from K-shell electrons. The XUV photons, with energies below about 1 keV, are emitted from plasma with temperatures between 10 and 150 eV, and result from bound-free processes. From photon energies between 0.5 and 1.5 keV continuum emission dominates.

To include radiation transport in the FP model, the source S_ν and absorption coefficient κ_ν must be specified. We take $S_\nu = S_\nu(z_c)f(z)$ with $f(z) = \exp(-(z - z_c)^2/L_c)$, where $S_\nu(z_c)$ is the radiation source. The absorption coefficient κ_ν consists of free-free, bound-free, and bound-bound processes. For a laser-produced aluminum plasma with laser intensity in the range of 10^{13}–10^{14} W/cm^2, the dominant (Duston *et al.*, 1983, 1985) absorption process consists of bound-free, free-free, and inner shell processes. The absorption coefficient can be written (More, 1986; Duston *et al.*, 1983, 1985) as $\kappa_\nu = \kappa_{\nu ff} + \kappa_{\nu bf}$ with

$$\kappa_{\nu bf} = \frac{8\pi}{\sqrt{27}}\frac{Q_n^4 P_n \alpha a_0^2 n_e}{n^5}\left(\frac{e^2}{a_0 h\nu}\right)^3(1 - f(\epsilon)), \tag{15}$$

where Q_n is the effective ion charge for shell n, a_0 is the Bohr radius, h is Planck's constant, α is the fine structure constant, P_n is the number of electrons in shell n, ν is the frequency, and f is the electron distribution function energy ϵ and

$$\kappa_{\nu ff} = \frac{16}{\sqrt{27}}\frac{\pi^2 Q^2 e^6 n_e n_i}{hcm_e^{3/2}T_e^{1/2}\nu^3}, \tag{16}$$

with T_e being the electron temperature, n_e being the electron density, n_i being the ion density, and m_e being the electron mass. The absorption cross-section for inner shell photoionization is taken from Duston *et al.* (1983). It is noted that $\kappa_{\nu bf} \simeq Q^4$. The total absorption cross-section for aluminum peaks in the photon energy regime of approximately 0.1–1 keV.

3. RESULTS

We have numerically solved the model equations consisting of Eqs. (3), (4), (13), (14), (15) with $f_2 = 0$. We have applied the model to a one-dimensional aluminum slab. The FP code is one-dimensional in space and two-dimensional in velocity space (v, $\eta = v_z/v$), with a Legendre polynomial expansion for η to an order of two. Self-consistent electric fields, electron-ion and electron-electron collisional effects, inverse bremsstrahlung absorption, and radiation transport are included in the model. Ion motion and other hydrodynamic transport effects are not included. The radiation source $S_\nu(z_c)$ is shown in Figure 1 for an aluminum plasma (Duston *et al.*, 1983). This source term is used as an initial

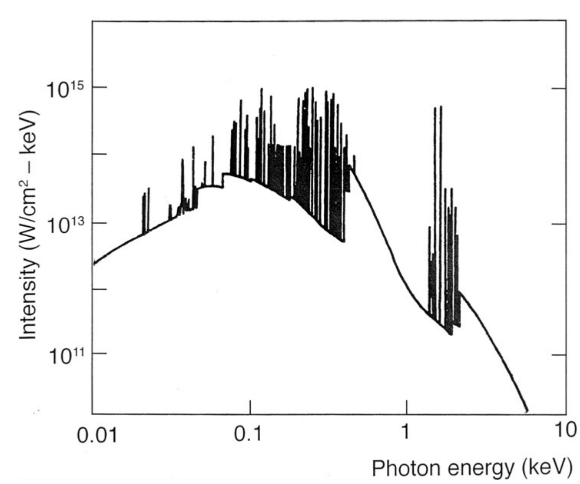

Fig. 1. Plot of radiation intensity for aluminum plasma for 1.06 μm laser with intensity of 10^{13} W/cm^2.

https://doi.org/10.1017/S0263034607000146 Published online by Cambridge University Press

condition in the FP code Eqs. (3)–(4). The scale size $L_c = 10\ \mu m$. The laser wavelength is 1.06 μm with intensity 10^{13}–10^{14} W/cm^2. Similar spectral intensities were also computed at shorter laser wavelengths of 0.35 μm for the same laser irradiance. The inverse bremsstrahlung S_{IB} and secondary radiation S_{rad} source terms are treated as time-independent in the solution of Eqs. (3)–(4).

Figure 2 shows the temperature and density at $t = 200$ ps with and without radiation transport. Without inclusion of radiation transport effects, it is found that the plasma temperature is overestimated in the critical region, and underestimated in the overdense plasma. This is due to the presence of radiative cooling in the critical region and radiative heating in the overdense region. Similar results were also obtained at the higher laser intensity of 10^{14} W/cm^2 and with different initial temperature and density profiles.

4. SUMMARY

In summary, radiation transport effects on FP nonlocal electron heat flow has been studied for aluminum laser-produced plasmas. It is found that, without radiation effects, the plasma temperature at the critical surface is underestimated and overestimated in the overdense plasma. The physical mechanism is due to a radiation-induced cooling at the critical layer and additional radiative heating in the overdense regions. It is concluded that, without radiation transport effects, the plasma temperature, as computed from FP models, is overestimated in the critical region and underestimated in the overdense region, for high-Z aluminum plasmas.

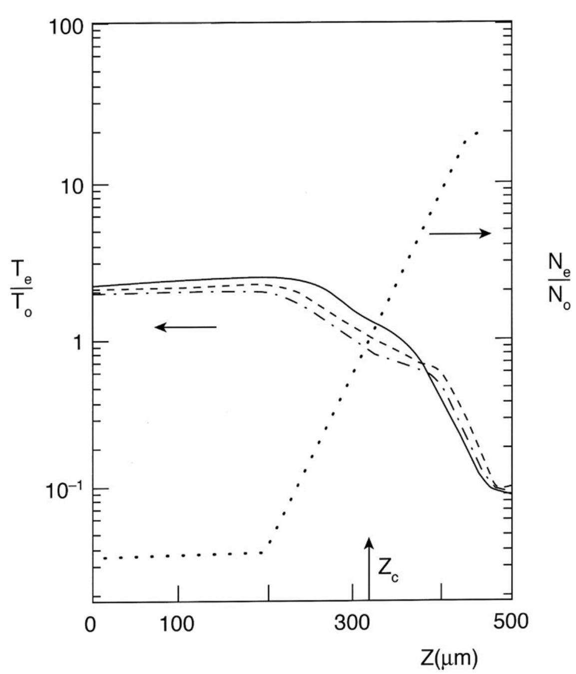

Fig. 2. Plot of temperature and density *vs.* z. Temperature plotted at $t = 200$ ps (solid line) without radiation transport and with radiation transport at $t = 105$ ps (dashed), $t = 200$ ps (dot-dashed). Density denoted by dotted line. Here $T_0 = 0.8$ keV and $N_0 = 10^{21}$ cm^{-3}.

ACKNOWLEDGMENTS

This work was supported by the U.S. Department of Energy. We thank Steve Obenschain, A. Velikovich, D. Fyfe, J. Gardner, S. Zalesak, D. Colombant, and W. Manheimer for useful discussions.

REFERENCES

Albritton, J. (1983). Laser absorption and heat transport by non-Maxwell-Boltzmann electron distributions. *Phys. Rev. Lett.* **50**, 2078.

Albritton, J., Williams, E., Bernstein, I.B. & Swartz, K.P. (1986). Nonlocal electron heat transport by not quite Maxwell-Boltzmann distributions. *Phys. Rev. Lett.* **57**, 1887.

Anwar, M., Latif, M., Iqbal, M.S., Rafique, M., Khaleeq-ur-rahman, M. & Siddique, S. (2006). Theoretical model for heat conduction in metals during interaction with ultra short laser pulse. *Laser Part. Beams* **24**, 347–353.

Bell, A. (1985). Non-Spitzer heat flow in a steadily ablating laser-produced plasma. *Phys. Fluids* **28**, 2007.

Bell, A.R., Evans, R.G. & Nicholas, D.J. (1981). Electron energy transport in steep temperature gradients in laser-produced plasmas. *Phys. Rev. Lett.* **46**, 243.

Bickerton, R.J. (1973). Thermal conduction limitations in laser fusion. *Nucl. Fusion* **13**, 457.

Duston, D., Clark, R.W., Davis, J. & Apruzese, J. (1983). Radiation energetics of a laser-produced plasma. *Phys. Rev. A* **27**, 1441.

Duston, D., Clark, R.W. & Davis, J. (1985). Effects of radiation on spectra, gradients, and preheat in laser-produced plasmas. *Phys. Rev. A* **31**, 3220.

Epperlein, E., Rickard, G.J. & Bell, A. (1988). Two-dimensional nonlocal electron transport in laser-produced plasmas. *Phys. Rev. Lett.* **61**, 2453.

Epperlein, E. & Short, R.W. (1991). A practical nonlocal model for electron heat transport in laser plasma. *Phys. Fluids B* **4**, 2211.

Epperlein, E. (1994). Fokker-Planck modeling of electron transport in laser-produced plasmas. *Laser Part. Beams* **12**, 257.

Fisher, D., Fraenkel, M., Zinamon, Z., Henis, Z., Moshe, E., Horovitz, Y., Luzon, E., Maman, S. & Eliezer, S. (2005). Intraband and interband absorption of femtosecond laser pulses in copper. *Laser Part. Beams* **23**, 391–393.

Gray, D. & Kilkenny, J. (1980). The measurement of ion acoustic turbulence and reduced thermal conductivity caused by a large temperature gradient in laser heated plasma. *Plasma Phys.* **22**, 81.

Griem, H.R. (1997). *Principles of Plasma Spectroscopy*. New York: Cambridge.

Key, M.H. (1985). Energy transport in laser plasmas. In *Laser Plasma Interactions* (Hooper M., Ed.) Vol. 3, pp. 143–157. New York: Edinburgh, Camelot Press.

Khalenkov, A.M., Borisenko, N.G., Kondrashov, V.N., Merkuliev, Y.A., Limpouch, J. & Pimenov, V.G. (2006). Experience of micro-heterogeneous target fabrication to study energy transport in plasma near critical density, *Laser part. Beams* **24**, 231–234.

Kruer, W.L. (1979). Laser plasma interactions. *Comm. Plasma Phys. Contro. Fusion* **5**, 69.

Lan, K., Feng, T.G., Lai, D.X., Xu, Y. & Meng, X.J. (2005). Study on two-dimensional transfer of radiating heating wave. *Laser Part. Beams* **23**, 275–282.

Langdon, A.B. (1980). Nonlinear inverse bremsstrahlung and heated distributions. *Phys. Rev. Lett.* **44**, 575.

Luciani, J., Mora, P. & Virmont, J. (1983). Nonlocal heat transport due to steep temperature gradients. *Phys. Rev. Lett.* **51**, 1664.

McClellan, G., Lee, P.H. & Caporaso, G. (1980). Z dependence of the laser-intensity threshold for inhibited electron thermal conduction. *Phys. Rev. Lett.* **44**, 658.

Malone, R.C., McCrory, R. & Morse, R.L. (1975). Indications of strongly flux-limited electron thermal conduction in laser target experiments. *Phys. Rev. Lett.* **34**, 721.

Manheimer, W. (1977). Energy flux limitation by ion acoustic turbulence in laser fusion schemes. *Phys. Fluids* **20**, 265.

Matte, J. & Virmont, J. (1982) Energy transport down steep temperature gradients. *Phys. Rev. Lett.* **49**, 1936.

Matte, J., Johnston, T.W., Delettrez, J. & McCrory, R.L. (1984). Electron heat transport with inverse bremsstrahlung and ion motion. *Phys. Rev. Lett.* **53**, 1461.

More, R.M. (1986). Radiation transport in laser plasmas. In *Laser Plasma Interactions* (Hooper M., Ed.) Vol. 3, pp. 243–259. New York: Edinburgh, Camelot Press.

Nakamura, T., Sakagami, H., Johzaki, T., Nagatomo, H. & Mima, K. (2006). Generation and transport of fast electrons inside cone targets irradiated by intense laser pulses. *Laser Part. Beams* **24**, 5–8.

Obenschain, S., Colombant, D., Karasik, M., Pawley, C., Serlin, V., Schmitt, A., Weaver, J., Gardner, J., Phillips, L., Aglitsky, Y., Chan, Y., Dahlburg, J.P. & Klapisch, M. (2002). Effects of thin high-Z layers on the hydrodynamics of laser-accelerated plastic targets. *Phys. Plasmas* **9**, 2234.

Petrov, Y. (2005). Energy exchange between the lattice and electrons in a metal under femtosecond laser irradiation. *Laser Part. Beams* **23**, 283–289.

Rickard, G.J., Bell, A. & Epperlein, E. (1989). 2D Fokker-Planck simulations of short-pulse laser-plasma interactions. *Phys. Rev. Lett.* **62**, 2687–2689.

Sherlock, M., Bell, A.R. & Rozmus, W. (2006). Absorption of ultra-short laser pulses and particle transport in dense targets. *Laser Part. Beams* **24**, 231–234.

Shkarofsky, I., Johnston, T. & Bachynski, M. (1966). *The Particle Kinetics of Plasmas*. Reading: Addison-Wesley.

Spitzer, L. & Harm, R. (1953). Transport phenomena in a completely ionized gas. *Phys. Rev.* **89**, 977.

Straus, M., Hazak, G., Shvarts, D. & Craxton, R.S. (1984). Magnetic field effects on electron heat transport in laser produced plasmas. *Phys. Rev. A* **30**, 2627.

Sunahara, A., Delettrez, J.A., Stoeckl, C., Short, R.W. & Skupsky, S. (2003). Time-dependent electron thermal flux inhibition in direc-drive implosions. *Phys. Rev. Lett.* **91**, 095003–1.

Xu, Y., Jiang, S., Lai, D.X., Pei, W.B., Ding, Y.K., Chang, T.Q., Lan, K., Li, S.G. & Feng, T. (2006). Two-photon group radiation transfer study in low density foam cylinder. *Laser Part. Beams* **24**, 495–501.

Yaakobi, B. & Bristow, T. (1977). Measurement of reduced thermal conduction in layered laser targets. *Phys. Rev. Lett.* **38**, 350.

Zel'dovich, Y. & Raizer, Y. (1966) *Physics of Shock Waves and High Temperature Hydrodynamic Phenomena*. New York: Academic.